IEEE Open Access Journal of
Power and Energy

Received 13 May 2020; revised 10 July 2020; accepted 12 July 2020. Date of publication 16 July 2020; date of current version 4 August 2020.

*Digital Object Identifier 10.1109/OAJPE.2020.3009684*

# Optimal Energy Dispatch of Distributed PVs for the Next Generation of Distribution Management Systems

**FEI DING[1] (Senior Member, IEEE), YINGCHEN ZHANG[1] (Senior Member, IEEE), JEFFERY SIMPSON[1], ANDREY BERNSTEIN[1] (Senior Member, IEEE), AND SUBRAMANIAN VADARI[2] (Senior Member, IEEE)**

[1]National Renewable Energy Laboratory, Golden, CO 80401 USA
[2]Modern Grid Solutions, Redmond, WA 98073 USA
CORRESPONDING AUTHOR: F. Ding (fei.ding@nrel.gov)

This work was supported by the U.S. DOE Office of Electricity under the Grid Modernization Laboratory Consortium GridAPPS-D Project.

**ABSTRACT** Advanced Distribution Management Systems (ADMS) are being widely adopted by electric utilities for managing and optimizing the operations of their distribution systems. Distributed photovoltaic (DPV) systems with smart inverters can be controlled to adjust active power and reactive power outputs, and they are envisioned to become a part of (centrally or distributed) controllable assets managed by the ADMS for optimizing grid operations. This paper proposes an optimal energy dispatch strategy controlling DPV systems for regulating distribution voltages and achieving conservation voltage reduction. A convex optimization model is proposed with the use of linearized power flow, and the gradient projection algorithm is used to solve the optimal active power and reactive power outputs of smart inverters. The proposed optimal energy dispatch is implemented using an open-source ADMS platform, and simulation results have demonstrated the effectiveness of the proposed approach on improving distribution grid operations.

**INDEX TERMS** Advanced distribution management system, distributed PV, smart inverter, voltage regulation, conservative voltage regulation, optimal power flow, volt-var control, volt-watt control.

## I. INTRODUCTION

WITH increasing electricity users' demands for higher reliability, power quality, renewable energy use, data security, and resilience, electric utilities are investing a variety of grid modernization technologies. Advanced distribution management system (ADMS) is a software platform that integrates numerous utility systems [1], including traditional distribution management system (DMS), supervisory control and data acquisition (SCADA), geographic information system, outage management system, meter data management system, etc., and provides a suite of different functionalities such as voltage optimization, state estimation, fault location, isolation, and service restoration. ADMS is expected to provide the full suite of distribution management and optimizations, and thus has been deploying at many utility territories to support these utilities to achieve their grid modernization objectives. Meantime, distributed energy resources, especially distributed photovoltaic (DPV) systems, are being widely integrated into distribution grids due to regulatory incentives and decreased costs [2], [3]. Although traditional DMS only manages legacy voltage regulating devices such as capacitor banks, transformer taps, and voltage regulators, it is widely accepted by vendors and utilities that ADMS should be aware of DPVs in the distribution system and be able to control them either directly or integrate with separate distributed energy resource management systems. In the past, due to the lack of enough situational awareness, DPVs are not commonly considered as the controllable assets by ADMS, and thus the optimal capability of DPVs for supporting distribution grid operations hasn't been well addressed. But technology maturity in solar forecasting and load forecasting has actually provided unique opportunity to develop advanced ADMS applications that can proactively dispatch the energy from DPVs in order to optimize grid operations.

Traditionally, DPVs are installed with standard inverters that only output real power. But today's inverters have improved dramatically into ''smart inverters'', which may

also be called ''advanced inverters''. Smart inverters can affect distribution grid voltages, currents and transformer loading significantly [4]–[7], and their existence in the distribution grid provides an alternative solution to improve grid operation without additional investment. Meantime, with the release of the updated distributed energy resource interconnection standard IEEE 1547-2018 [8], DPVs in the United States, either utility-owned or behind-the-meter assets incentivized by grid service signals [9], are expected to become part of utilities' operation strategies in helping regulate both distribution voltage and frequency by altering their active and reactive power outputs.

At present, most of existing PV inverters in the field are using autonomous volt-var control and volt-watt control. The pre-defined voltage-reactive power and voltage-active power piecewise functions are provided for each inverter, and the inverter detects its local voltage and determines its reactive power (or active power) output based on the piecewise function. This method doesn't require advanced communications or optimizations, and the inverter can respond to voltage changes instantaneously. Both simulation results and field tests have proved the effectiveness of local autonomous inverter control on improving distribution feeder voltage profiles and power quality [10]–[15]. Besides, some literatures have also proposed different optimization methods to optimize the parameters used in the piecewise function. The work in [16] leverages an extremum seeking approach to develop local rules for the update of reactive setpoints. The paper [17] focuses on proportional control strategies where the active and reactive output-powers of DERs are adjusted in response to (and proportionally to) local changes in voltage levels. In [18], a centralized parameter tuning model of control curves is built, in which Q-V and Pcurtailment-V curves of PV inverters are formulated using piecewise linearization, and the optimal curves are determined by solving a mixed-integer second-order cone programming optimization model. However, given the local response nature, a system-wide coordination is lacked, and it is impossible to guarantee the satisfaction of global objectives when providing utility grid services.

On the other hand, network-wide optimal power flow (OPF) approaches were developed to optimally control PV reactive power output and active power curtailment [19]. Recently a unified real-time OPF model was proposed in [20], and it leverages massive system measurements as feedback and can solve the optimization problem in a distributed and online manner. However, considering currently most utilities do not have enough sensing and communication devices to support such heavy data exchange in real time, we inherited the OPF model proposed in [20], but revised it to solve the offline optimization problem without relying on real-time measurements as feedback. Besides, realistic models and constraints for both DPVs and utility distribution grids are included in the paper to solve different voltage optimization objectives. In addition, under a U.S. Department of Energy Grid Modernization Laboratory Consortium effort, an open-source, standards-based platform – GridAPPS-D [21] has been developed to enable the development and deployment of advanced ADMS applications considering realistic data communication. GridAPPS-D provides an open source development platform for distribution energy management applications. The platform emphasizes standard based approach to enable the applications interoperability. This approach ensures applications developed under this platform be running for variety of distribution networks and distribution energy management systems. The platform provides futuristic data rich and control rich environment for applications that are future facing but may not be able to be implemented in current software systems. In addition to algorithm development and simulation validations, we have also implemented the proposed control architecture using the GridAPPS-D platform, and the codes developed to support the application will be published in GitHub in the future.

Compare with the aforementioned PV dispatch methods, this manuscript presents a linear OPF based approach that is unique in the follow aspects.

1. This proposed method optimizes both active and reactive set-points implicitly in the linearization. In order to solve the non-convexity of real and reactive power, both real and reactive power operation point and constraints are included in the linearization process.
2. The proposed method uses gradient projection algorithm to solve the convex optimization after linearization efficiently, and accurately avoiding the requirement of massive measurement feedbacks.
3. The proposed method is implemented in a realistic operation system framework for testing, with data bus handling inputs and outputs, the algorithm's realistic remanence can be evaluated.

The remaining of the paper is organized as follows. Section II describes the optimization model and algorithm for solving optimal power setpoints for PV inverters. Section III presents the proposed DPV control architecture to provide grid services. Section IV lists the test system and all scenarios to study. Multiple simulation studies and result analyses are provided in Section V, and conclusions are summarized in Section VI.

## II. OPTIMAL ENERGY DISPATCH OF DPV SYSTEMS

### A. OPTIMIZATION MODEL

The proposed optimal energy dispatch problem aims at solving the optimal active power and reactive power outputs for smart PV inverters in order to satisfy different distribution grid operation objectives while minimizing PV curtailment. Also, reactive power output minimization is considered in the objective function in order to avoid unnecessary reactive current circulation in the inverter. It is worth noting that although voltage optimization is studied solely in the paper, the proposed optimization model can be used to control different types of distributed energy resources (e.g., battery inverters, controllable loads, etc.) to fulfill different distribution grid operation objectives such as peak demand management and frequency regulation.

Two types of voltage optimization are considered in the paper: 1) Voltage regulation can be enabled by enforcing the constraint that requires all node voltages to satisfy ANSI Range A limit [22], i.e. 0.95-1.05 pu, or other preferred voltage bounds. 2) Conservation voltage reduction is a method of lowering utilization voltages on a circuit to conserve energy consumptions [23]. It is achieved in the proposed optimization model by adding minimizing voltage deviation from the allowed minimum voltage, *i.e.,* 0.95 pu, into the objective function.

Then, the objective function and voltage constraint are formulated as:

$$\min_{p_j^t q_j^t} f(\mathbf{x^t}) = \sum_{t=t_0}^{t_0+\Delta t} \left( \sum_{j=1}^{N_{PV}} \left[ c_j^P \cdot \left( p_j^{t,max} - p_j^t \right)^2 + c_j^Q \cdot \left( q_j^t \right)^2 \right] + \sum_{k=1}^{N_{LD}} c_k^v \cdot \left( v_k^t - 0.95 \right)^2 \right)$$
$$s.t. \underline{v} \le \left| v_k^t \right| \le \overline{v}, \quad \forall k \in N \tag{1}$$

where, $\mathbf{x^t} = \left\{ p_j^t, q_j^t, j = 1, \ldots, N_{PV} \right\}$, and $p_j^t$ and $q_j^t$ are active power output and reactive power output from the $j^{th}$ PV inverter at time $t$. $t_0$ and $t_0 + \Delta t$ defines the operational time horizon. $p_j^{t,max}$ is the maximum active power output that can be generated from the $j^{th}$ PV inverter at time $t$. $v_k^t$ is node-$k^{th}$ voltage at time $t$. $\underline{v}$ and $\overline{v}$ are respectively lower and upper voltage limits. $N_{PV}$, $N_{LD}$ and $N$ are the total number of distributed PV inverters under control, total number of load locations under CVR measurement, and total number of nodes in the feeder respectively. $c_j^P$, $c_j^Q$, and $c_j^v$ are constant coefficients, and their values could be inputs from PV owners or determined depending on applications. Specifically, when CVR is not implemented, $c_j^v$ is enforced to be 0.

PV inverter operation should follow the industry practice, which is limiting the amount of reactive power to be 44% of the inverter capacity in order to restrict inverter power factor higher than 0.9. It is common in the industry to oversize the PV array by using a DC-to-AC (kW) ratio of around 1.15 in order to utilize the system components to their full capacity [24]. Legacy PV inverters do not oversize the inverter, but it becomes common to oversize smart inverters in order to retain reactive power support capability during the peak PV generation time. Since PV inverters are expected to provide reactive power support for satisfying the emerging grid service request from utilities, it is reasonable to assume that PV systems adopt night mode operation, i.e. inverters can still provide reactive power support at night when there is no PV array power generation. Thus, the feasible solution set for $p_j^t$ and $q_j^t$ is defined as

$$\chi^t = \begin{cases} 0 \le p_j^t \le p_j^{t,max} \\ \left( p_j^t \right)^2 + \left( q_j^t \right)^2 \le S_j^2 \\ \left( q_j^t \right)^2 \le 0.44^2 \cdot S_j^2 \\ S_j = P_j^{DC} / 1.15 \cdot \alpha_{inv} \end{cases} \tag{2}$$

where, $S_j$ and $P_j^{DC}$ are respectively the inverter size and DC panel size for the $j^{th}$ PV system. $\alpha_{inv}$ is the inverter AC kW to kVA ratio.

Voltages in distribution systems are inherently nonlinear function of loads and generations, and the nonlinearity of three-phase unbalanced power flow equations poses significant challenges for the development of computationally affordable optimization solutions. Approximated linear power flow models have been widely used to facilitate the development of computationally efficient optimization approaches. Similarly, this paper leverages the linear power flow model proposed in [25] to solve voltages for the three-phase unbalanced distribution network. Complex voltages ($\mathbf{V}$) and voltage magnitudes ($|\mathbf{V}|$) for all the nodes excluding slack buses can be modeled as the linear functions of node power injections, as

$$\mathbf{V} = \mathbf{\Phi_P} \cdot \mathbf{P_{bus}} + \mathbf{\Phi_Q} \cdot \mathbf{Q_{bus}} + \boldsymbol{\varphi} \tag{3}$$
$$|\mathbf{V}| = \mathbf{\Psi_P} \cdot \mathbf{P_{bus}} + \mathbf{\Psi_Q} \cdot \mathbf{Q_{bus}} + \boldsymbol{\omega} \tag{4}$$

where, $\mathbf{P_{bus}}$ and $\mathbf{Q_{bus}}$ are respectively active power injection vector and reactive power injection vector at feeder nodes. $\mathbf{\Phi_P}$, $\mathbf{\Phi_Q}$, $\mathbf{\Psi_P}$ and $\mathbf{\Psi_Q}$ are power coefficient matrices for the linear power flow model, and $\boldsymbol{\varphi}$ and $\boldsymbol{\omega}$ are constant vectors. According to the fixed-point linearization proposed in [22], the values of $\mathbf{\Phi_P}$, $\mathbf{\Phi_Q}$, $\mathbf{\Psi_P}$, $\mathbf{\Psi_Q}$, $\boldsymbol{\varphi}$ and $\boldsymbol{\omega}$ can be calculated as

$$\mathbf{\Phi_P} = \mathbf{Y_{11}^{-1}} \cdot \mathrm{diag}\left( \hat{\mathbf{V}}^* \right)^{-1} \tag{6.a}$$
$$\mathbf{\Phi_Q} = -\mathbf{j} \mathbf{Y_{11}^{-1}} \cdot \mathrm{diag}\left( \hat{\mathbf{V}}^* \right)^{-1} \tag{6.b}$$
$$\mathbf{\Psi_P} = \left| \mathrm{diag}\left( \boldsymbol{\varphi} \right) \right| \cdot \Re \left\{ \mathrm{diag}\left( \boldsymbol{\varphi} \right)^{-1} \cdot \mathbf{Y_{11}^{-1}} \cdot \mathbf{diag}\left( \hat{\mathbf{V}}^* \right)^{-1} \right\} \tag{6.c}$$
$$\mathbf{\Psi_Q} = \left| \mathrm{diag}\left( \boldsymbol{\varphi} \right) \right| \cdot \Re \left\{ -\mathbf{j} \cdot \mathrm{diag}\left( \boldsymbol{\varphi} \right)^{-1} \cdot \mathbf{Y_{11}^{-1}} \cdot \mathbf{diag}\left( \hat{\mathbf{V}}^* \right)^{-1} \right\} \tag{6.d}$$
$$\boldsymbol{\varphi} = -\mathbf{Y_{11}^{-1}} \cdot \mathbf{Y_{10}} \cdot \mathbf{V_0} \tag{6.e}$$
$$\boldsymbol{\omega} = |\boldsymbol{\varphi}| \tag{6.f}$$

where, $\mathbf{\Phi_P}$, $\mathbf{\Phi_Q}$, $\mathbf{\Psi_P}$ and $\mathbf{\Psi_Q}$ are all $N \times N$ matrices, and $\boldsymbol{\varphi}$ and $\boldsymbol{\omega}$ are both $N \times 1$ vectors. $\hat{\mathbf{V}}$ is the given solution to linear voltage and $(\cdot)^*$ is the conjugate of the complex value. $\mathbf{V_0}$ is the voltage vector for slack buses, and the bus that connects to the substation is considered as slack bus. R$\cdot\}$ is the real part of a complex value. $\mathbf{Y_{11}}$ and $\mathbf{Y_{10}}$ are matrix elements of the node admittance matrix ($\mathbf{Y_{bus}}$) that correlates current injections and voltages at feeder nodes as:

$$\begin{bmatrix} \mathbf{I_0} \\ \mathbf{I} \end{bmatrix} = \begin{bmatrix} \mathbf{Y_{00}} & \mathbf{Y_{01}} \\ \mathbf{Y_{10}} & \mathbf{Y_{11}} \end{bmatrix} \cdot \begin{bmatrix} \mathbf{V_0} \\ \mathbf{V} \end{bmatrix} \tag{7}$$

As a result, we can covert (2) into the following two linear constraints:

$$\begin{cases} g_k\left( \mathbf{x^t} \right) = \sum_{j=1}^{N} \psi_P^{kj} \cdot p_j^t + \sum_{j=1}^{N} \psi_Q^{kj} \cdot q_j^t + \omega_k - \overline{v} \le 0 \\ h_k\left( \mathbf{x^t} \right) = \underline{v} - \sum_{j=1}^{N} \psi_P^{kj} \cdot p_j^t + \sum_{j=1}^{N} \psi_Q^{kj} \cdot q_j^t + \omega_k \le 0 \end{cases} \tag{8}$$

where, $\psi_P^{kj}$, $\psi_Q^{kj}$ and $\omega_k$ are the matrix elements for $\mathbf{\Psi_P}$, $\mathbf{\Psi_Q}$, $\boldsymbol{\omega}$ respectively.

Finally, the optimal energy dispatch of DPVs can be formulated as the following convex optimization problem.

$$\begin{aligned} &\min_{p_j^t q_j^t \in \chi^t} f(\mathbf{x^t}) \\ &s.t.\ g_k\left(\mathbf{x^t}\right) \le 0, \quad k = 1, \ldots, N \\ &\quad h_k\left(\mathbf{x^t}\right) \le 0, \quad k = 1, \ldots, N \end{aligned} \tag{9}$$

### B. ALGORITHM

The gradient projection algorithm [26], [27] can be used to solve the proposed convex optimization problem defined by (9). Define the Lagrangian of the optimization problem at time $t$ as

$$\mathrm{L}\left(\mathbf{x_t}, \bar{\boldsymbol{\mu}}_\mathbf{t}, \underline{\boldsymbol{\mu}}_\mathbf{t}\right) = f\left(\mathbf{x^t}\right) + \sum_{k=1}^{N} \bar{\mu}_k^t \cdot g_k\left(\mathbf{x^t}\right) + \sum_{k=1}^{N} \underline{\mu}_k^t \cdot h_k\left(\mathbf{x^t}\right) \tag{10}$$

Then, at each time slot $t$, decision variables $\mathbf{x_t}$ and Lagrange multipliers $\bar{\boldsymbol{\mu}}_\mathbf{t}$ and $\underline{\boldsymbol{\mu}}_\mathbf{t}$ are updated iteratively until the Karush-Kuhn-Tucker (KKT) conditions are satisfied. For each iteration $i$, we can obtain:

$$\mathbf{x_i^t} = \mathrm{Proj}\left\{\mathbf{x_{i-1}^t} - \alpha_x \cdot \nabla_x \mathcal{L}(\mathbf{x_{i-1}^t}, \bar{\boldsymbol{\mu}}_\mathbf{i-1}^\mathbf{t}, \underline{\boldsymbol{\mu}}_\mathbf{i-1}^\mathbf{t})\right\} \tag{11}$$

$$\begin{cases} \bar{\boldsymbol{\mu}}_\mathbf{i}^\mathbf{t} = \mathrm{Proj}\left\{\bar{\boldsymbol{\mu}}_\mathbf{i-1}^\mathbf{t} + \alpha_{\bar{\mu}} \cdot \nabla_{\bar{\mu}} \mathcal{L}(\mathbf{x_{i-1}^t}, \bar{\boldsymbol{\mu}}_\mathbf{i-1}^\mathbf{t}, \underline{\boldsymbol{\mu}}_\mathbf{i-1}^\mathbf{t})\right\} \\ \underline{\boldsymbol{\mu}}_\mathbf{i}^\mathbf{t} = \mathrm{Proj}\left\{\underline{\boldsymbol{\mu}}_\mathbf{i-1}^\mathbf{t} + \alpha_{\underline{\mu}} \cdot \nabla_{\underline{\mu}} \mathcal{L}(\mathbf{x_{i-1}^t}, \bar{\boldsymbol{\mu}}_\mathbf{i-1}^\mathbf{t}, \underline{\boldsymbol{\mu}}_\mathbf{i-1}^\mathbf{t})\right\} \end{cases} \tag{12}$$

where, $\alpha_x$, $\alpha_{\bar{\mu}}$,$\alpha_{\underline{\mu}}$ are constant stepsizes, and $\nabla_x \mathcal{L}$, $\nabla_{\bar{\mu}} \mathcal{L}$ and $\nabla_{\underline{\mu}} \mathcal{L}$ are the projected gradients.

Notably, through the iterative updates, without the need of using real-time system measurement as feedback, we can still solve the optimal active power and reactive power setpoints of DPVs with appropriate values of stepsizes and enough number of iterations. For practical applications, it might be inevitable to get a tradeoff between the global optimality and better computational efficiency. As a result, a small number of iterations can be used but this can still yield a satisfied DPV control performance on improving grid operations. This will be proved via simulation analysis later in the paper.

From (10), we can find that the updates of individual Lagrangian multiplier $\bar{\mu}_k^t$ and $\underline{\mu}_k^t$ depends on the calculations of $g_k\left(\mathbf{x^t}\right)$ and $h_k\left(\mathbf{x^t}\right)$, which can be easily computed using (8) but require system-wise topology information reflected by linear power flow coefficient matrices $\mathbf{\Psi_P}$, $\mathbf{\Psi_Q}$, $\boldsymbol{\omega}$. It is noted that these coefficient matrices should be updated if system topology gets changed.

**TABLE 1. Optimal energy dispatch Algorithm for PV inverters.**

| |
|---|
| Compute matrices $\mathbf{\Psi_P}$, $\mathbf{\Psi_Q}$, $\boldsymbol{\omega}$ using (6). Re-computation is required if system topology gets reconfigured. |
| At time $t$: |
| let i =1 |
| while $\|\mathbf{x_i^t} - \mathbf{x_{i-1}^t}\|_2 > \varepsilon$ do: |
| "Coordinator": |
| a) compute $\nabla_{\bar{\mu}}\mathcal{L}$ and $\nabla_{\underline{\mu}}\mathcal{L}$ based on $\mathbf{x_{i-1}^t}, \bar{\boldsymbol{\mu}}_\mathbf{i-1}^\mathbf{t}, \underline{\boldsymbol{\mu}}_\mathbf{i-1}^\mathbf{t}, \mathbf{\Psi_P}$, $\mathbf{\Psi_Q}$, and $\boldsymbol{\omega}$ using (8) and (10); |
| b) solve $\bar{\boldsymbol{\mu}}_\mathbf{i}^\mathbf{t}$ and $\underline{\boldsymbol{\mu}}_\mathbf{i}^\mathbf{t}$ using (12); |
| c) solve $\sum_{k=1}^N \bar{\mu}_k^t \cdot \nabla_x g_k(\mathbf{x_{i-1}^t})$ and $\sum_{k=1}^N \underline{\mu}_k^t \cdot \nabla_x h_k(\mathbf{x_{i-1}^t})$ based on $\bar{\boldsymbol{\mu}}_\mathbf{i-1}^\mathbf{t}, \underline{\boldsymbol{\mu}}_\mathbf{i-1}^\mathbf{t}, \mathbf{\Psi_P}$ and $\mathbf{\Psi_Q}$ using (8). |
| For each of total $N_{PV}$ "Local Action Makers": denote its decision variable as $p$ and $q$. Then, |
| a) compute $\nabla_p f(p_{i-1}^t)$ and $\nabla_q f(q_{i-1}^t)$; |
| b) acquire the two single values $\sum_{k=1}^N \bar{\mu}_k^t \nabla_p g_k(p_{i-1}^t) + \sum_{k=1}^N \underline{\mu}_k^t \nabla_p h_k(p_{i-1}^t)$ and $\sum_{k=1}^N \bar{\mu}_k^t \nabla_q g_k(q_{i-1}^t) + \sum_{k=1}^N \underline{\mu}_k^t \nabla_q h_k(q_{i-1}^t)$ from the Coordinator; |
| c) compute $\nabla_p \mathcal{L}$ and $\nabla_q \mathcal{L}$, and update $p_i^t$ and $q_i^t$. |
| let i=i+1; |
| obtain $\mathbf{x_t^*} = \mathbf{x_i^t}$. |

On the other hand, the calculation of gradient $\nabla_x \mathcal{L}$ for updating decision variables $\mathbf{x^t}$ is achieved by:

$$\nabla_x \mathcal{L}\left(\mathbf{x_{i-1}^t}, \bar{\boldsymbol{\mu}}_\mathbf{i-1}^\mathbf{t}, \underline{\boldsymbol{\mu}}_\mathbf{i-1}^\mathbf{t}\right) = \nabla_x f\left(\mathbf{x_{i-1}^t}\right) + \sum_{k=1}^{N} \bar{\mu}_k^t \cdot \nabla_x g_k\left(\mathbf{x_{i-1}^t}\right) + \sum_{k=1}^{N} \underline{\mu}_k^t \cdot \nabla_x h_k\left(\mathbf{x_{i-1}^t}\right) \tag{13}$$

It is obvious that the first term at the right side of the above equation only require local DPV information and can be easily calculated from (1). But calculating the last two terms require the knowledge of all Lagrangian multipliers and matrices $\mathbf{\Psi_P}$, $\mathbf{\Psi_Q}$. As a result, we can design solving the optimization problem (9) as a distributed approach that consists of two hierarchical layers. The procedure is described as Table I.

## III. CONTROL ARCHITECTURE FOR ADMS APPLICATIONS

Based on the above optimization model, we propose a control architecture and its implementation using the GridAPPS-D platform, depicted in Fig. 1, to coordinately optimize smart inverter outputs of DPVs for the applications in future ADMS products. The control architecture consists of three components:

1) System Information Acquisition – gathers system information including topology, locations and sizes of PV systems, and system contingencies (such as network reconfiguration, fault). All the information is necessary to compute linear power flow model coefficients and formulate the optimization problem.

2) Monitoring and Prediction – measures PV inverter power output and receives AMI and SCADA measurements in a regular frequency. These measurements are used as the initialization inputs $\mathbf{x_0^t}$ and $\mathbf{v_0^t}$ for the optimal control.

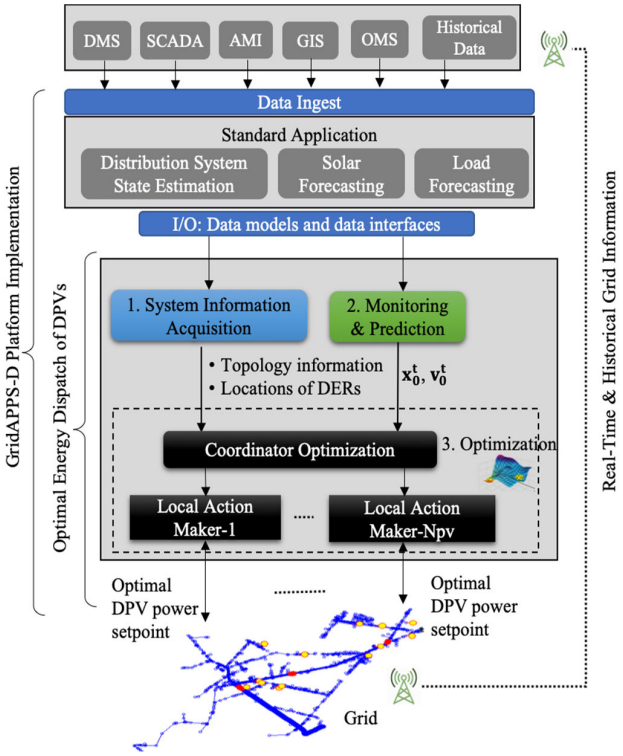


**FIGURE 1.** **The proposed control architecture using DPV systems to improve distribution grid operation.**

Besides, voltage measurements are always evaluated to monitor whether voltage violations exist, and if so, the ''Optimization'' will be activated automatically to adjust the outputs of controlled DPVs to mitigate voltage issues. On the other hand, the predicted solar irradiance is acquired to compute $p_j^{t,max}$ and the predicted load power is also obtained, and all the prediction information are used to proactively solve the optimal active power and reactive power outputs of DPVs.

3) Optimization – solves the optimal power setpoints for PV inverters based on the process described in Table I, and sends the optimal setpoints to the controlled DPVs in the grid. It is noted that the computations involved are simple and do not rely on any commercial solvers, and the solutions can be solved fast. Thus, the proposed optimization model can be well applied in the real-time ADMS operations.

To demonstrate how the proposed control architecture can be applied for ADMS applications, we have implemented the optimal energy dispatch of DPVs using the GridAPPS-D platform. GridAPPS-D is a common software platform that delivers standardized operational technology integration, enabling accelerated development and deployment of portable applications for power system planning and operations. As shown in Figure 1, the GridAPPS-D platform receives and integrates data from commercial DMS, SCADA, advanced metering infrastructure (AMI), geographic information system (GIS), and outage management system (OMS). These data, together with the estimated system data provided by distribution system state estimation service inside the GridAPPS-D platform,

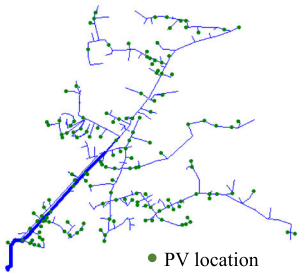


**FIGURE 2.** **K1 feeder topology and the locations of PV systems.**

and forecasted solar and load data provided by standard applications, are sent to the designed control architecture and used for solving the proposed DPV energy dispatch problem. Details about the application programming interfaces for GridAPP-D implementation can refer to [28]. Also, it worth noting that when outage or other contingency happens in the grid, the OMS should inform the application and system information acquisition component will re-extract system topology information for solving its updated optimization decisions.

## IV. CASE STUDY

### A. TEST SYSTEM

The proposed optimal energy dispatch of DPVs is validated on the K1 feeder [29] — a moderate-size, real utility system in southeastern of the United States. The K1 feeder models both medium-voltage and low-voltage circuits. In total 1747 nodes and 320 three-phase and single-phase loads are modeled, and one controllable LTC and one non-controllable capacitor also exist in the model. The use of K1 feeder demonstrating realistic distribution feeder size can provide convincing results for validating both control convergency and scalability of the proposed approach. In this paper, 150 DPVs are added into the K1 feeder, reaching to 90% of peak load penetration. The locations of PV systems and feeder topology are depicted in Fig. 2.

Besides, Fig. 3 shows one-day normalized load and PV profiles, which represent a moderate-to-high loading condition and an intermittent solar irradiance. The data resolution is 1 minute.

### B. AUTONOMOUS SMART INVERTER CONTROLS

Autonomous Volt/VAR and Volt/Watt controls are two default control modes for smart inverters required by IEEE 1547-2018. The former regulates the reactive power output of the smart inverter based on its local voltage by following a voltage-reactive power piecewise linear characteristic (e.g. Volt/VAR curve), while the latter regulates (curtails) the active power output of the smart inverter by following a volt/Watt curve. The proposed optimal energy dispatch of DPVs will be compared with the autonomous inverter control, and the approved Volt/VAR curve and proposed Volt/Watt curve by Hawaiian Electric Company [12] are used in the

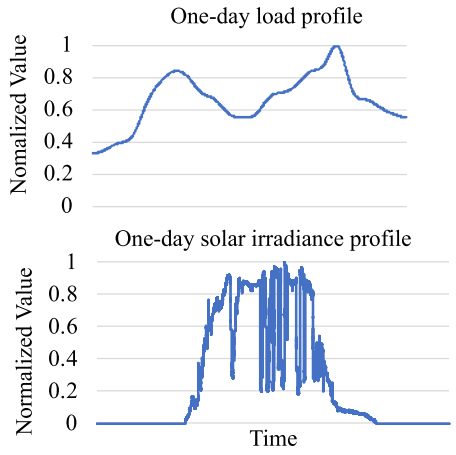


**FIGURE 3.** One-day load profile and PV profile.

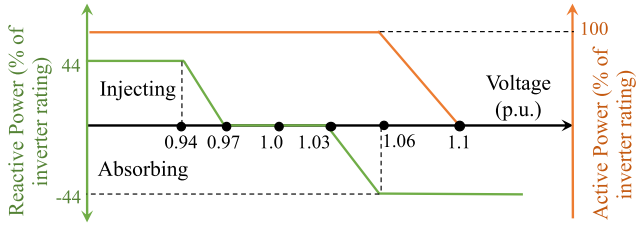


**FIGURE 4.** Autonomous smart inverter control.

following section to model the autonomous inverter control. As depicted in Fig. 4, the maximum reactive power (e.g. 44% of inverter size) will be injected into the grid when voltage is below 0.94 pu, while consumed when voltage is over 1.06 pu. No reactive power is producing when voltage is between 0.97 and 1.03 pu. The smart inverter starts curtailing active power when voltage exceeds 1.06 pu and will shut down when voltage reaches to 1.1 pu.

### C. SCENARIOS

Table 2 summarizes the scenarios that are studied in the paper. Note that although the proposed optimal energy dispatch solves its problem using the linear power flow model, the solutions are sent and applied in the OpenDSS feeder model [26] running under quasi-static time-series (QSTS) simulations, and the results generated below are all obtained from the real power flow results provided by the OpenDSS simulation, which thus represents real responses of the grid.

### D. RESULTS

Simulation results of the above scenarios will be presented based on QSTS simulations, and they will be used to prove the effectiveness of the proposed DPV energy dispatch approach on improving distribution grid voltages. In addition, the convergency performance of the proposed optimization algorithm is first demonstrated by using a snapshot simulation.

#### 1) ALGORITHM PERFORMANCE

Fig. 5 and Fig. 6 respectively shows the result of system voltages and optimal DPV power setpoints obtained during

**TABLE 2.** Simulation scenarios.

| Scenario | Description |
|---|---|
| S-0 | All DPVs operate under unity power factor |
| S-1 | Optimal energy dispatch of all 150 DPVs to regulate all load bus voltages to be within Range A |
| S-2 | Optimal energy dispatch of all 150 DPVs to regulate all load bus voltages to be within 0.97 and 1.03 pu |
| S-3 | Optimal energy dispatch of all 150 DPVs to lower load bus voltages and achieve CVR |
| S-4 | Autonomous inverter control implemented for all 150 DPVs following the curve in Fig. 3 |
| S-5 | Optimal energy dispatch of only 50 DPVs to regulate all load bus voltages to be within Range A |
| S-6 | Optimal energy dispatch of only 100 DPVs to regulate all load bus voltages to be within Range A |

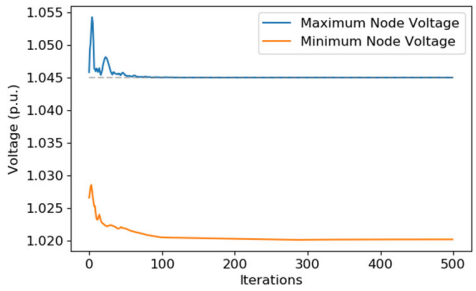


**FIGURE 5.** The convergency of system voltage at one time snapshot after 500 iterations.

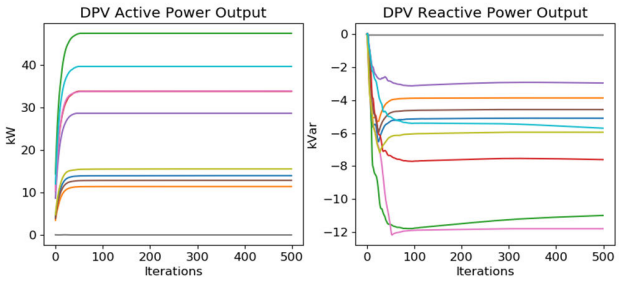


**FIGURE 6.** The convergency of DPV power setpoints (active power – left, reactive power – right) at one time snapshot after 500 iterations.

one time snapshot study with 500 iterations. It can be found that the proposed algorithm can converge very fast, generally less than 200 iterations – taking only around 5 seconds using a computer with 3.5 GHz Intel Core i7. This proves that the proposed DPV energy dispatch approach fits well for the real-time ADMS implementations that typically operate every 5-15mins.

#### 2) GRID PERFORMANCE IMPACT

*a: Impact of DPVs on providing distribution grid service*

Fig. 7 shows one-day load bus voltage ranges, defined by the maximum, minimum and median values, respectively

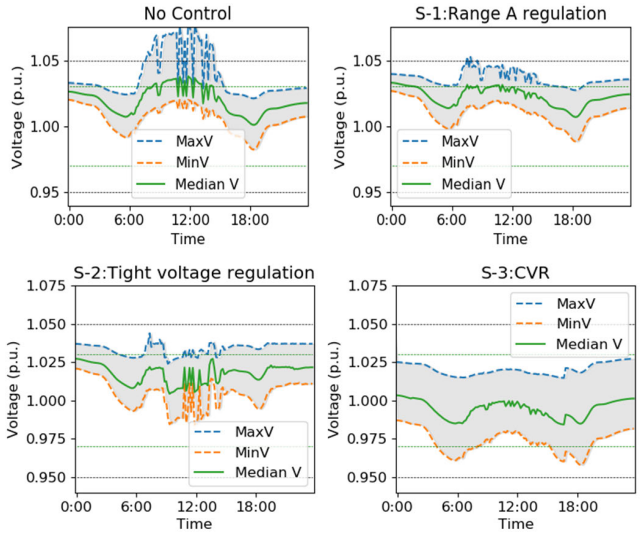


**FIGURE 7.** One-day voltage range for scenarios 0-3.

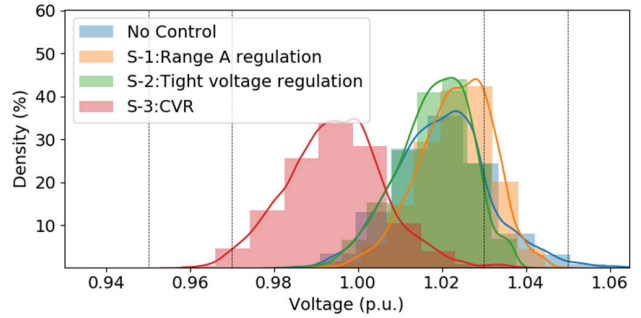


**FIGURE 8.** The distribution of all load voltages during one day for scenarios 0-3.

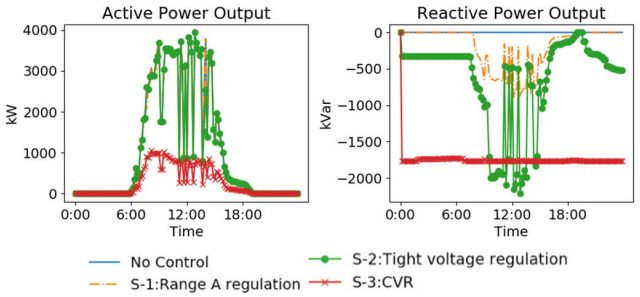


**FIGURE 9.** DPV inverter power outputs for scenarios 0-3.

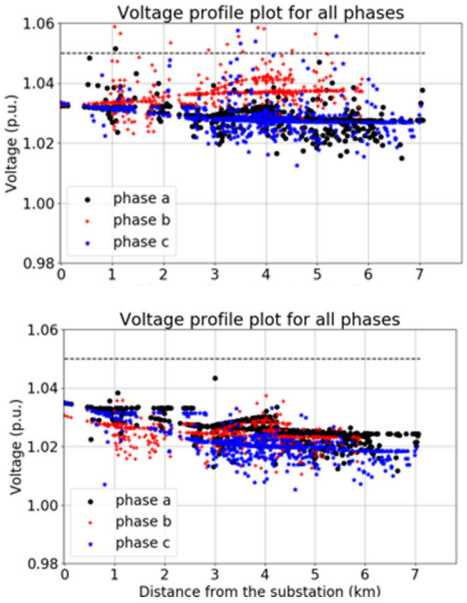


**FIGURE 10.** Three-phase voltage profiles at 12:10 pm compared between S-0 (top) and S-1 (bottom).

obtained for scenarios S-0, S-1, S-2 and S-3. Compared with S-0, S-1 result shows that all load bus voltages can be regulated to be always within Range A limit, and S-2 result shows that load bus voltages can be further restricted to be below 1.04 pu. S-3 result shows that when CVR is implemented, the maximum load voltage is always around 1.03 pu and the minimum voltage is around 0.95 pu. Moreover, Fig. 8 compares the distribution of all load voltages during one day for the four scenarios. The results show that the voltage profile obtained in S-3 is shifted to be closer to 0.95 pu compared with S-0 voltage due to the voltage reduction objective included in the optimization model, and S-2 voltage becomes tighter than S-1.

Accordingly, Fig. 9 shows the results of inverter power outputs for the four scenarios. Compared with S-0, active power outputs of DPVs in S-1 do not curtail at all, and voltage regulation is achieved only by adjusting the reactive power output. In S-2, active power outputs get slightly curtailed at some moments, and more reactive power is consumed than S-1 in order to further reduce voltage to 1.03 pu. In S-3, a lot of active power from DPVs is curtailed during the daytime, and reactive power is always consumed significantly in order to reduce load voltages.

In addition, all node voltages along with the distances from the substation at 12:10 pm are compared between S-0 and S-1, shown as Fig. 10. With the proposed DPV energy dispatch, system voltages become much tighter and always lie in the desired range.

### *b: Controlling subset of DPV inverters*

Because the proposed control architecture relies on DPVs to regulate distribution voltage and implement advanced grid support, the geographic locations and quantities of DPVs directly affect the controllability and thus alter the control effectiveness. As a result, the voltage results and PV power outputs are compared between scenarios S-1, S-5 and S-6. Fig. 11 shows that the voltage ranges obtained in S-5 and S-6. Compared with the S-1 result shown in Fig. 5, the voltages are still exceeding 1.05 pu during 9 am and 2 pm.

Besides, Fig. 12 shows the active power and reactive power outputs from the controlled DPVs, and both S-5 and S-6 have

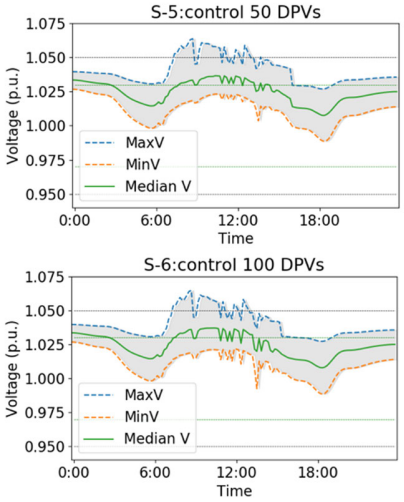


FIGURE 11. **One-day voltage range for scenarios S-5 and S-6.**

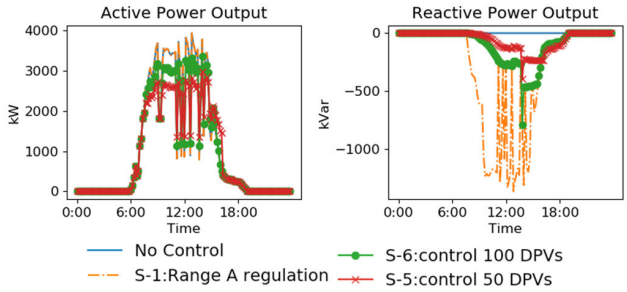


FIGURE 12. **DPV inverter power outputs for scenarios S-0, S-1, S-5 and S-6.**

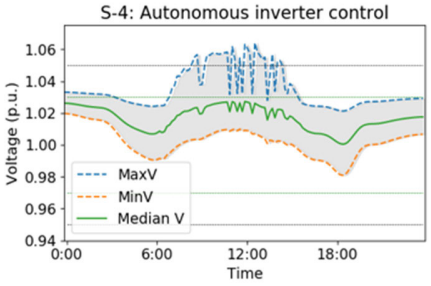


FIGURE 13. **One-day voltage range for scenario S-4.**

active power curtailment because the reactive power support from the limited controllable DPVs doesn't have enough capability to reduce voltages to be below 1.05 pu.

*c: Coordinated DPV control v.s. autonomous inverter control*

Fig. 13 shows the voltage range obtained in S-4. Compared with the S-0 result shown in Fig. 7, the use of autonomous inverter control can mitigate overvoltage, however, different from S-4 result, it couldn't eliminate all overvoltages. Fig. 14 compares inverter power outputs between S-1 and S-4. Active power from DPVs doesn't need to be curtailed based

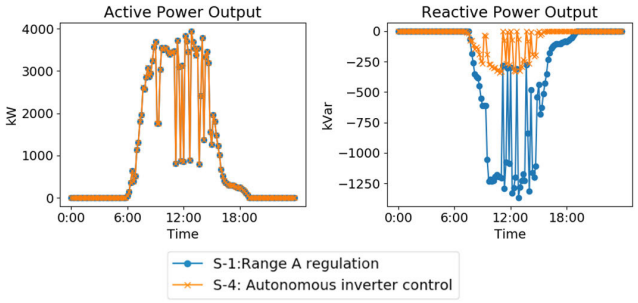


FIGURE 14. **DPV inverter power outputs for scenarios S-1 and S-4.**

on the autonomous volt-watt curve design. And, reactive power consumed by smart inverters is much less than S-1, which explains why overvoltage still exists in S-4. This is because autonomous inverter control only monitors local inverter voltages, and the inverters that do not see overvoltage will not provide much reactive power or even provides zero reactive power support if their local voltages are inside the Volt/VAR curve deadband.

## V. CONCLUSION

This paper proposes an optimal energy dispatch strategy for distributed PV systems in order to optimize distribution voltages and provide grid services. A convex optimization model is proposed with the use of linearized power flow, and the gradient projection algorithm is used to solve the optimal active power and reactive power of smart inverters. The proposed optimization model can coordinately control both utility-scale PVs and distributed residential PVs, and use these resources to regulate distribution voltages and conserve energy consumptions. Besides, the proposed optimal energy dispatch of DPVs aligns with the open-source GridAPPS-D framework and is expected to be an advanced ADMS application for emerging distribution grids with high penetration of PVs.

## ACKNOWLEDGEMENT

The views expressed in the article do not necessarily represent the views of the DOE or the U.S. Government. The U.S. Government retains and the publisher, by accepting the article for publication, acknowledges that the U.S. Government retains a nonexclusive, paid-up, irrevocable, worldwide license to publish or reproduce the published form of this work, or allow others to do so, for U.S. Government purposes.

## REFERENCES

[1] U.S. Department of Energy. (Feb. 2015). *Voices of Experience: Insights Into Advanced Distribution Management Systems*. [Online]. Available: https://www.energy.gov/sites/prod/files/2015/02/f19/Voices%20of%20Experience%20-%20Advanced%20Distribution%20Management%20Systems%20February%202015.pdf

[2] B. Palmintier *et al.*, "On the path to SunShot: Emerging issues and challenges in integrating solar with the distribution system," Nat. Renew. Energy Lab., Golden, CO, USA, Tech. Rep. NREL/TP-5D00-65331, 2016.

[3] K. Horowitz, F. Ding, B. Mather, and B. Palmintier, "The cost of distribution system upgrades to accommodate increasing penetrations of distributed photovoltaic systems on real feeders in the United States," Nat. Renew. Energy Lab., Golden, CO, USA, Tech. Rep. NREL/TP-6A20-70710, 2018.

[4] J. Seuss, M. J. Reno, R. J. Broderick, and S. Grijalva, "Improving distribution network PV hosting capacity via smart inverter reactive power support," in *Proc. IEEE Power Energy Soc. General Meeting*, Jul. 2015, pp. 1–5.

[5] M. H. J. Bollen and A. Sannino, "Voltage control with inverter-based distributed generation," *IEEE Trans. Power Del.*, vol. 20, no. 1, pp. 519–520, Jan. 2005.

[6] *Stochastic Analysis to Determine Feeder Hosting Capacity for Distributed Solar PV*, Electr. Power Res. Inst., Palo Alto, CA, USA, 2012, Art. no. 1026640.

[7] F. Ding and B. Mather, "On distributed PV hosting capacity estimation, sensitivity study, and improvement," *IEEE Trans. Sustain. Energy*, vol. 8, no. 3, pp. 1010–1020, Jul. 2017.

[8] *IEEE Standard for Interconnection and Interoperability of Distributed Energy Resources With Associated Electric Power Systems Interfaces*, IEEE Standard 1547-2018, Feb. 2018.

[9] *Definitions, Standards and Test Procedures for Grid Services from Devices, DOE Grid Modernization Initiative Peer Review*, Standard GMLC 1.4.2, Apr. 2017.

[10] F. Ding *et al.*, "Voltage support study of smart PV inverters on a high-photovoltaic penetration utility distribution feeder," in *Proc. IEEE 43rd Photovolt. Spec. Conf. (PVSC)*, Portland, OR, USA, Jun. 2016, pp. 1–5.

[11] F. Ding *et al.*, "Application of autonomous smart inverter volt-VAR function for voltage reduction energy savings and power quality in electric distribution systems," in *Proc. IEEE PES ISGT Conf.*, Washington, DC, USA, Apr. 2017, pp. 1–5.

[12] J. Giraldez *et al.*, "Simulation of Hawaiian electric companies feeder operations with advanced inverters and analysis of annual photovoltaic energy curtailment," Nat. Renew. Energy Lab., Golden, CO, USA, Tech. Rep. NREL/TP-5D00-68681, Sep. 2017.

[13] R. K. Varma, S. S. Rangarajan, I. Axente, and V. Sharma, "Novel application of a PV solar plant as STATCOM during night and day in a distribution utility network," in *Proc. IEEE/PES Power Syst. Conf. Exposit.*, Phoenix, AZ, USA, Mar. 2011, pp. 1–8.

[14] S. S. Rangarajan, E. R. Collins, and J. C. Fox, "Smart PV and Smart-Park inverters as suppressors of TOV phenomenon in distribution systems," *IET Gener., Transmiss. Distrib.*, vol. 12, no. 22, pp. 5909–5917, Dec. 2018.

[15] S. A. Raza and J. Jiang, "A benchmark distribution system for investigation of residential microgrids with multiple local generation and storage devices," *IEEE Open Access J. Power Energy*, vol. 7, pp. 41–50, 2020.

[16] D. B. Arnold, M. Negrete-Pincetic, M. D. Sankur, D. M. Auslander, and D. S. Callaway, "Model-free optimal control of VAR resources in distribution systems: An extremum seeking approach," *IEEE Trans. Power Syst.*, vol. 31, no. 5, pp. 3583–3593, Sep. 2016.

[17] K. Baker, A. Bernstein, E. Dall'Anese, and C. Zhao, "Network-cognizant voltage droop control for distribution grids," *IEEE Trans. Power Syst.*, vol. 33, no. 2, pp. 2098–2108, Mar. 2018.

[18] H. Ji *et al.*, "A centralized-based method to determine the local voltage control strategies of distributed generator operation in active distribution networks," *Appl. Energy*, vol. 228, pp. 2024–2036, Oct. 2018.

[19] X. Su, M. A. S. Masoum, and P. J. Wolfs, "Optimal PV inverter reactive power control and real power curtailment to improve performance of unbalanced four-wire LV distribution networks," *IEEE Trans. Sustain. Energy*, vol. 5, no. 3, pp. 967–977, Jul. 2014.

[20] E. Dall'Anese and A. Simonetto, "Optimal power flow pursuit," *IEEE Trans. Smart Grid*, vol. 9, no. 2, pp. 942–952, Mar. 2018.

[21] R. B. Melton *et al.*, "Leveraging standards to create an open platform for the development of advanced distribution applications," *IEEE Access*, vol. 6, pp. 37361–37370, 2018.

[22] *American National Standard for Electric Power Systems and Equipment—Voltage Ratings (60 Hz)*, Standard ANSI C84.1-2016, 2016.

[23] F. Ding and M. Baggu, "Coordinated utilization of smart inverters with legacy voltage control devices in distribution systems with high distributed PV penetration—Increase CVR energy savings," *IEEE Trans. Smart Grid*, early access, Jul. 18, 2018, doi: 10.1109/TSG.2018.2857410.

[24] P. Grana. *Solar Inverters and Clipping: What DC/AC Inverter Load Ratio is Ideal?* Accessed: Jul. 8, 2016. [Online]. Available: https://www.solarpowerworldonline.com/2016/07/solar-inverters-clipping-dcacinverter-load-ratio-ideal/

[25] A. Bernstein and E. Dall'Anese, "Linear power-flow models in multiphase distribution networks," in *Proc. IEEE PES Innov. Smart Grid Technol. Conf. Eur. (ISGT-Europe)*, Turin, Italy, Sep. 2017, pp. 1–6.

[26] W. Zhang, Y. Ma, W. Liu, S. J. Ranade, and Y. Luo, "Distributed optimal active power dispatch under constraints for smart grids," *IEEE Trans. Ind. Electron.*, vol. 64, no. 6, pp. 5084–5094, Jun. 2017.

[27] L. Gan and S. H. Low, "An online gradient algorithm for optimal power flow on radial networks," *IEEE J. Sel. Areas Commun.*, vol. 34, no. 3, pp. 625–638, Mar. 2016.

[28] Battelle Memorial Institute. *GridAPPS-D's Documentation*. [Online]. Available: https://gridappsd.readthedocs.io/en/master/

[29] Electric Power Research Institute, Inc. *Feeder K1*. [Online]. Available: https://dpv.epri.com/feeder_k.html